Information Transfer in a Sinus Node Cell Model

T. BIEBERLE, B. HENSEL, M. SCHALDACH
Department of Biomedical Engineering, University of Erlangen-Nuremberg, Erlangen, Germany

Summary

Instabilities in cardiovascular autonomic control play an important role in the genesis of atrial or ventricular tachyarrhythmias. Since changes in autonomic tone produce changes in heart rate variability, it has been suggested that heart rate variability be used for a stability analysis of cardiovascular autonomic control. We investigated the importance of the sinus node in this scenario by analyzing the information transfer in a numerical single cell model previously introduced by Dokos. Vagal activity is simulated through the release of bursts of acetylcholine. These bursts are characterized by their phase f with respect to the cellular action potential, the number of acetylcholine releases per burst, and the delay between subsequent releases. During continued vagal stimulation at constant parameters, the cycle length of the action potential increases linearly over a wide range of the delay or the number of stimuli (constant phase, constant delay). If the total burst duration is kept constant, the cycle length exhibits a strong non-linear dependence on the number of stimuli per burst. The cycle length increases monotonically with increases in the phase shift. For values of $f > 0.29$ s, oscillations in the cycle length are observed. We modulated the burst parameters with a time series generated by integrating the Mackey-Glass equation, and calculated the correlation dimension of the cycle lengths in order to see whether the information on the dynamic of vagal activity is conserved in the cycle lengths. It turned out that the dynamics of the original time series may be entirely reconstructed in those areas of parameter space where the cycle length exhibits a linear dependence on the parameters. Reconstruction is impaired in those regions where the cycles length exhibits a non-linear dependence on the parameters. Thus, we concluded that, in general, the dynamics of cardiovascular autonomic control may not be reconstructed from the cycle lengths because the dynamic characteristics of the sinus node are superimposed.

Key Words

Cell model, sinus node, correlation dimension

Introduction

Today, it is generally appreciated that imbalances in cardiovascular autonomic control play an important role in the genesis of atrial or ventricular tachyarrhythmias. Reduced vagal tone or increased sympathetic tone are associated with an increased risk for ventricular tachycardia. There is evidence that atrial fibrillation may be promoted by both enhanced parasympathetic or sympathetic activity in selected patient populations. It would therefore be highly desirable to deduce markers for prospective risk stratification from a stability analysis of cardiovascular autonomic control [1]. However, direct measurement of the autonomic tone is not possible. It has been shown, however, that the variability of the cardiac cycle length depends on autonomic activity [2]. Thus, vagal tone is associated with a peak between 0.15 and 0.4 Hz in the power spectral density of the RR intervals, whereas sympathetic activity is expected to result in a maximum of between 0.04 and 0.15 Hz [1]. The urgent need for a non-invasive, easy applicable method for prospective risk strat-

ification has stimulated numerous investigations on heart rate variability. These studies have revealed controversial results, however. The early hypothesis that the presence or absence of vagal protection is the only relevant factor has not been confirmed. Ultralow frequency components of the power spectral density and even depressed sympathetic HRV components seem to have predictive power with respect to survival after myocardial infarction [3]. Thus, one may conclude that information on the stability of cardiovascular autonomic control is encoded in the cardiac cycle lengths in a rather complex way.

On the other hand, the electrophysiologic processes underlying heart rate variability have never been analyzed with respect to the information transfer from autonomic control to the cardiac cycle length. The sinoatrial node, atrioventricular node, conduction system, and myocardium are known to be innervated by sympathetic and parasympathetic nerves, and heart rate increases or decreases following stimulation of the respective nerves have been demonstrated in experimental and numerical models. However, it has never been investigated whether these processes conserve the information on cardiovascular autonomic control. If information is lost, it is not possible to unambiguously reconstruct the dynamics of the autonomic nervous system using the cardiac cycle length, and methods based on dynamics reconstruction, such as fractal dimension or entropy, must fail. We therefore raised the question of whether the dynamics of the cardiovascular autonomic control can be mapped one-to-one onto the cardiac cycle length.

As mentioned above, it is not possible to directly assess the integral level of the autonomic tone. Thus, one might be inclined to investigate the map from autonomic dynamics onto cardiac cycle length in subsystems where autonomic activity is accessible. In animal experiments, for example, the parasympathetic nerves have been stimulated directly to study the effect of this on the blood pressure and cardiac cycle length (cf. [4]). While this approach provided valuable insight under steady state conditions, it would not be useful for studying dynamic effects, since compensatory effects of other parts of the autonomic control cannot be eliminated under experimental conditions. This methodological problem may be avoided by using a numerical description of the mapping from cardiovascular autonomic control onto cardiac cycle length. The numerical approach has the additional advantage that the boundary conditions may be kept constant, which would be very difficult to ensure during experimental investigations.

The cyclic activity of the heart stems from the spontaneous formation of transmembrane action potentials in the cells of the sinoatrial node. The electric excitation then spreads from the sinus node across the atria and passes through the atrioventricular node and the ventricular conduction system, until eventually the ventricular muscle is activated, causing a contraction. Thus, the sinus node is the natural starting point for a systematic investigation of the information transfer from the cardiovascular autonomic control to the cardiac cycle length. In the following, we will analyze the information transfer using the model of a single, vagally driven sinus node cell that was introduced by Dokos et al. in 1996 [5,6]. A time-delayed differential equation with well-known dynamic behavior, the so-called Mackey-Glass equation, will be used to modulate vagal activity [7]. Then, the dynamic of the cellular cycle length will be analyzed and compared to the original dynamic.

Materials and Methods

Brief Review of the Cell Model

The Dokos model of the rabbit sinus node cell is based on the approach introduced in 1951 by Hodgkin and Huxley, who described the cell membrane as an electrical network of the transmembrane capacitance and several conductive elements representing the different currents of sodium, potassium, and calcium ions [8]. The conductive elements are described by means of time- and voltage-dependent gate variables that are assumed to follow a first-order kinetic. In the Dokos cell model, this approach leads to 18 coupled differential equations that are integrated using a fourth order Runge-Kutta method [9]. The model comprises seven passive transmembrane currents, the Na^+/K^+ pump current, the Na^+/Ca^{2+} exchange current and the calcium uptake and release in the sarcoplasmic reticulum [5].

Vagal activity is included through the burst release of acetylcholine (ACh) from a main storage into the neuroeffector junctions and into the extrajunctional space. The ACh concentration is assumed to rise instantaneously following the release. From the extrajunctional space, the acetylcholine is transported via a diffusion-limited process to the neuroeffector junctions. There, it activates the potassium current $i_{K,\,ACh}$ via fourth- order kinetics and modulates the hyperpolar-

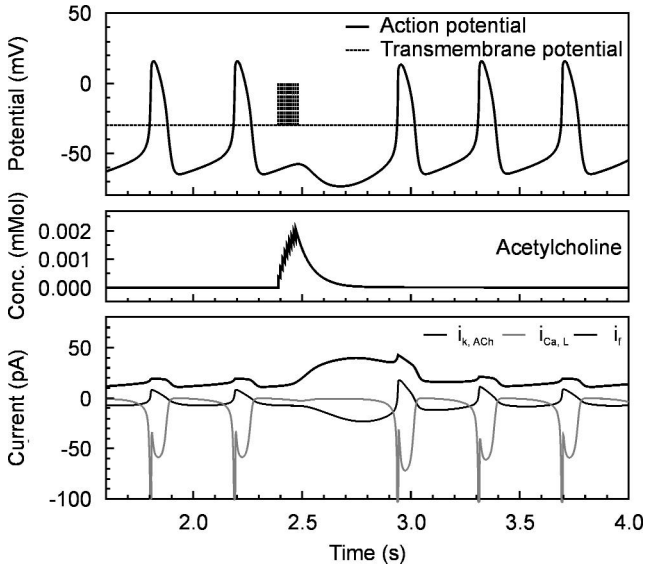

Figure 1. Effect of vagal stimulation on the potassium current ($i_{K, ACh}$), the hyperpolarization activated current (i_f), and the L-type calcium current ($i_{Ca, L}$). The net effect on the transmembrane potential is a hyperpolarization that delays the subsequent action potential upstroke.

ization activated current i_f and the L-type calcium current $i_{Ca, L}$ [6]. Figure 1 visualizes the effect of a burst release of acetylcholine (ten stimuli) on these currents. The net effect on the transmembrane potential consists in hyperpolarization and a delay of the subsequent upstroke in the action potential.

Obviously, the effect of vagal stimulation depends on the number *n* of stimuli per burst. However, it also depends on the timing of the burst within the cellular cycle. Therefore, the level of vagal activity is also characterized by the phase *f* of the first stimulus with respect to the cellular cycle and by the delay *d* of subsequent stimuli within one burst. Since the interplay of these three parameters is not known, two of them were always kept fixed while the remaining one was modulated with the Mackey-Glass system. Note, however, that it is intrinsically impossible to keep the *mean* phase of the burst fixed while varying the number of stimuli or the delay. Any change in these parameters will simultaneously result in a shift in the mean phase.

Non-linear System Analysis

In our model studies, we used a time-delayed non-linear differential equation, that was originally introduced by Mackey and Glass for describing the generation of blood cells [7]:

$$\dot{x} = \frac{ax(t-\theta)}{1+(x(t-\theta))^n} \qquad \text{(Equation 1).}$$

Equation 1 was integrated using a fourth order Runge-Kutta method with parameter values of a = 0.2, b = 0.1, n = 10, and θ = 17. The resulting time series were used to modulate vagal activity in the cell model. Then the correlation dimension of the cycle lengths was estimated and compared to the correlation dimension of the original time series.

The correlation dimension is a measure of the complexity of the trajectory of non-linear dynamic systems in phase space. It was defined by Grassberger and Procaccia as [10]

$$D_2 = \lim_{\varepsilon \to 0} \frac{\log C(\varepsilon)}{\log \varepsilon} \qquad \text{(Equation 2)}$$

where the C(ε) is the correlation integral

$$C(\varepsilon) = \lim_{N \to \infty} \frac{1}{N^2} \sum_{i,j=1}^{N} H\left(\varepsilon - \left|x_i - x_j\right|\right) \qquad \text{(Equation 3).}$$

The Heaviside function H is defined as

$$H(\alpha) = \begin{cases} 0 \text{ for } \alpha < 0 \\ 1 \text{ for } \alpha \geq 0 \end{cases} \qquad \text{(Equation 4).}$$

Thus, the correlation integral C(ε) is the number of points in phase space with a distance of less than ε from some reference point. The correlation dimension is equivalent to the topological dimension of regularly shaped objects, i.e., the correlation dimension of a line is one and the correlation dimension of a square is two. However, for irregularly shaped objects, the correlation dimension assumes non-integer values and thus allows for a more subtle characterization of the complexity of geometric objects or of trajectories in phase space.

The multi-dimensional phase space of a non-linear dynamic system may be reconstructed out of the time series of one single system variable by taking advantage of Taken's theorem on time-delayed co-ordinates [11]. The time-delayed coordinates of a time series x(t) are defined as

$$y(t) = \{x(t), x(t+\tau), \ldots, x(t+(m-1)\cdot\tau)\} \qquad \text{(Equation 5).}$$

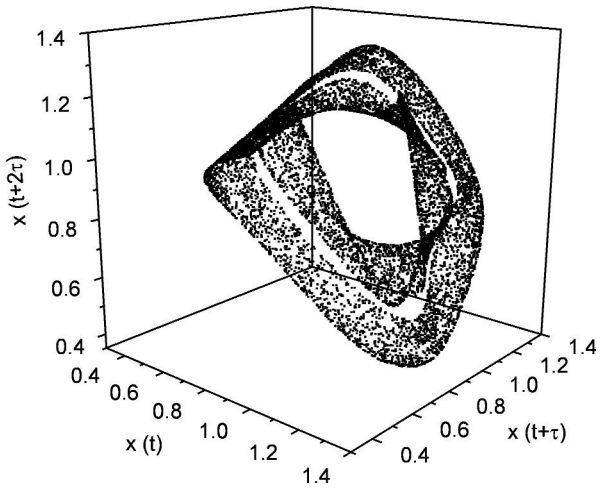

Figure 2. 3D embedding space of the Mackey-Glass system (m = 3, and t = 10).

Figure 2 shows an embedding space of the Mackey-Glass system with m = 3, and τ = 10. The theorem states that the map defined in equation 5 is an embedding of the system dynamics, if the embedding dimension $m > 2 D_2 + 1$. This means that for high values of *m*, the time-delayed co-ordinates are equivalent to the phase space of the system. This theorem thus allows the reconstruction of the phase space for both the original Mackey-Glass time series and the resulting series of cellular cycle lengths. The correlation dimension is then estimated iteratively for increasing embedding dimension m by calculating the slope in the plot of log C(ε) over log ε (Equation 2 suggests that there should be a linear scaling region in the log-log plot). Figure 3 displays the plots of the correlation integral and the resulting values of the slope for the original Mackey-Glass time series. Note that with an increasing embedding dimension *m*, the slope saturates against the value of the correlation dimension $D_2 = 1.942 \pm 0.002$.

Results and Discussion

Simulations with Constant Parameters for Vagal Stimulation

The investigation of the information transfer implies the application of continued vagal stimulation, i.e., acetylcholine is released in every cellular cycle. Since the effect of a vagal burst does not decay immediately, the following burst encounters different conditions and consequently has a different effect on the transmembrane currents. If the burst parameters remain unchanged, eventually a steady state is achieved. This behavior is visualized in Figure 4, where the phase of the vagal burst has been increased every 600 cycles. It is most prominent in the beginning after vagal stimulation has been turned on. Note that for values of the phase 0.29 s < ϕ < 0.37 s, the cycle length oscillates even in the steady state between several values rather than assuming one single value. This observation may be explained by the latency of the effect of the vagal burst on the transmembrane potential: for high values of the phase, the burst does not affect the action potential that immediately follows it, but rather the second

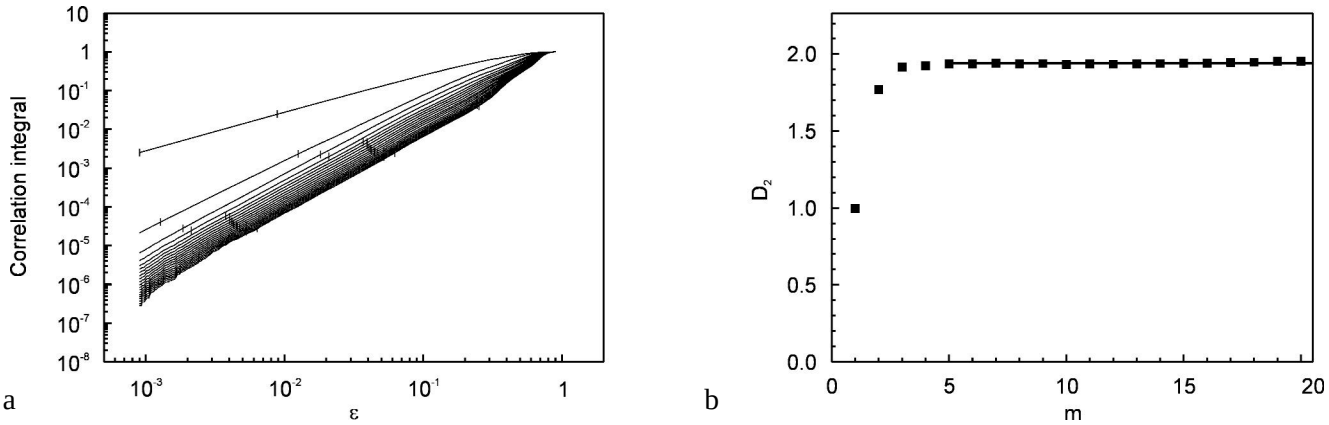

Figure 3. a) Correlation integrals of the original Mackey-Glass time series. b) Slope values as determined from Panel a. The slope saturates against the correlation dimension $D_2 = 1.942 \pm 0.002$.

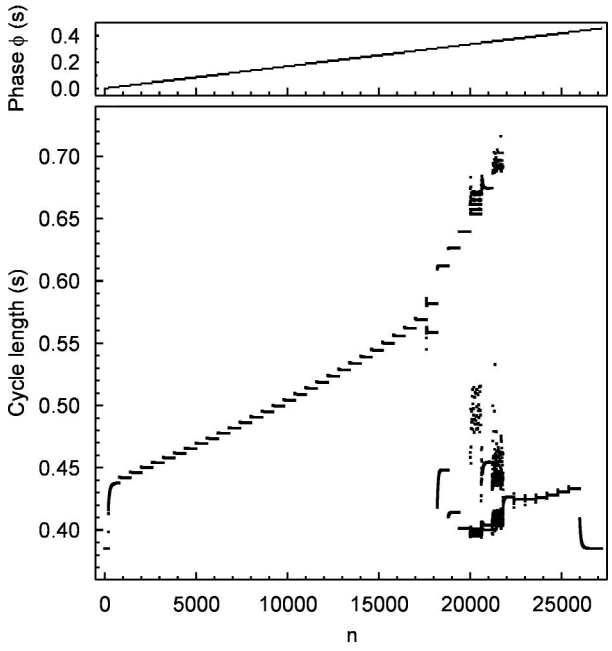

Figure 4. Time series of the cycle length, where the phase f of the vagal burst is increased every 600 cycles. Note the oscillations of the cycle length for values of the phase 0.29 s < f < 0.37 s.

potential. This second action potential is then delayed by the summed effect of two stimuli, whereas the third potential is again influenced by only one vagal burst; thus, the cycle length oscillates.

The relationship between the cycle length and the delay *d* of subsequent stimuli within the burst is less complex: the cycle length increases linearly with an increasing delay *d*. Keeping the phase ϕ and the delay *d* constant while varying the number of stimuli leads to the rather peculiar situation that the cycle length varies in discrete steps rather than as a smooth function. Obviously, such stepwise changes are completely unphysiologic, and they have indeed not been observed in any experimental or clinical investigation. The real sinus node consists of a large number of cells which are not homogeneously innervated and which exert entrainment effects on each other. In order to take into account the averaging effect that results from this behavior, we reduced the amount of acetylcholine per stimulus in our simulations. Figure 5 displays the cycle length as a function of the number of stimuli per burst. In Figure 5a, the delay *d* between consecutive stimuli was kept constant, whereas in Figure 5b the total duration of the burst was kept constant, i.e., both the number of stimuli and the delay were varied. During constant delay, the relationship between the cycle length and the number of stimuli is linear over almost the whole range, whereas during constant total duration, the cycle length is a curvilinear function of the number of stimuli.

Simulations with Dynamic Modulation of the Parameters of Vagal Stimulation

All simulations in this chapter have been executed with the same input time series. The Mackey-Glass equation was integrated for a = 0.2, b = 0.1, n = 10, and θ = 17 with a step size of 0.01. The resulting time series was sampled with a delay time of τ = 10 and scaled accord-

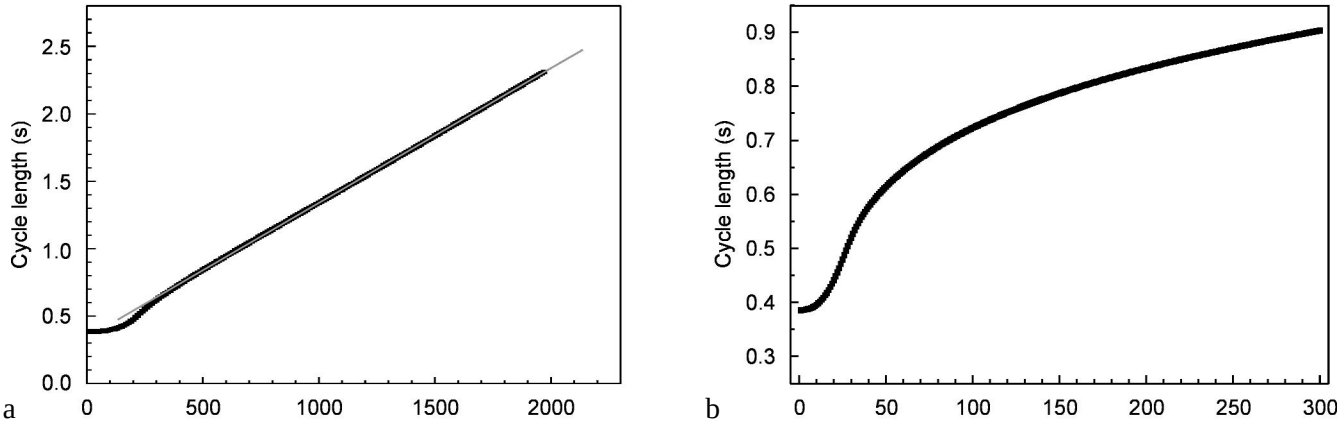

Figure 5. Cycle length as a function of the number n of stimuli per burst at constant delay (a) and at constant total duration of the burst (b).

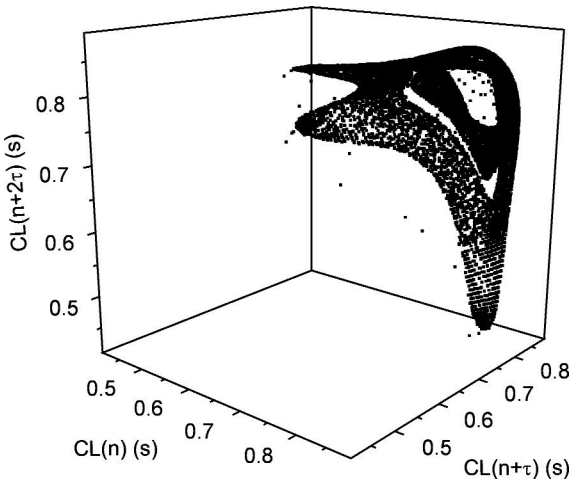

Figure 6. 3D embedding space of the cycle lengths (CL), when the number n of stimuli per burst is modulated by the Mackey-Glass time series (constant burst phase f = 0.1 s and constant total burst duration d_{total} = 0.3 s). The attractor is distinctly distorted as compared to the original one in Figure 2.

ing to the value range of the parameter to be modulated. This approach ensures that the simulation uses the entire dynamic range of the modulated parameter, and avoids offset effects.

The investigations during steady state situations as described above have revealed a rather complex relationship between the parameters of vagal stimulation and the resulting cycle length. The information transfer in the sinus node cell thus may be affected by oscillations and non-linearities, depending on the parameter that is modulated. In addition, it has been shown that hysteresis effects influence the cycle length during vagal stimulation, i.e., the effect of a stimulus indeed depends on the parameters of the previous one. It is therefore quite remarkable that vagal activity can be mapped one-to-one on the cycle length, if the parameters that led to a linear dependence of the resulting cycle lengths during steady state simulations are modulated: If the delay between subsequent stimuli is modulated with the Mackey-Glass time series (constant phase ϕ = 0.2 s and number of stimuli n = 5), the correlation dimension of the cycle lengths of D_2 = 1.943 ± 0.001 is nearly identical to the value assumed for the original time series: D_2 = 1.942 ± 0.002. Also modulation of the number of pulses per burst (constant phase ϕ and delay d = 0.001 s) has only marginal influence on the scaling behavior of the trajectory: D_2 = 1.989 ± 0.002. Thus, the hysteresis effects observed during steady state conditions do not seem to play a role during dynamic modulations.The situation changes, however, in those simulations where the cycle length does not depend linearly on the modulated input parameter. Figure 6 displays the 3D embedding space of the cycle lengths, where the number n of stimuli per burst is modulated by the Mackey-Glass time series (constant

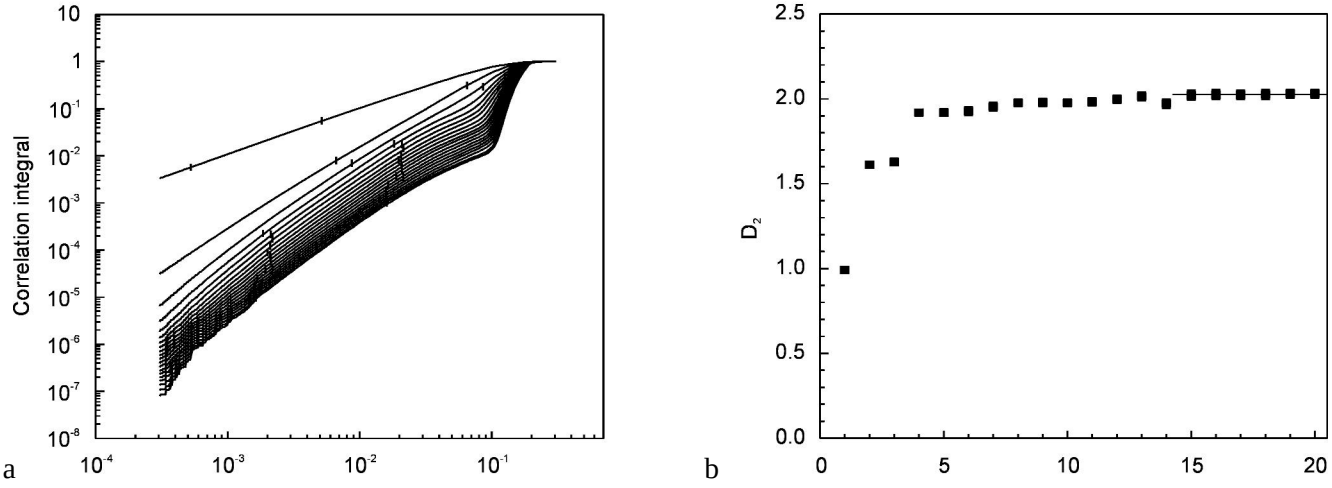

Figure 7. a) Correlation integrals of the cycle lengths, where the number n of stimuli per burst is modulated by the Mackey-Glass time series (one pulse per "burst"). b) Slope values calculated. Saturation occurs rather late and at a value higher than in the original system (D_2 = 2.027 ± 0.002; for m > 15).

burst phase $\phi = 0.1$ s and constant total burst duration $d_{total} = 0.3$ s). The attractor still consists of two interwoven bands of points. However, the edges are prolonged in the direction of the co-ordinate axes. The correlation integrals do not exhibit a linear scaling region, hence it is not possible to determine a correlation dimension.

The results are similar if the phase ϕ is modulated with the Mackey-Glass time series during a constant number of pulses per "burst" of n = 1. The oscillations and the discontinuity revealed by Figure 4 lead to heavy distortions in the embedding space of the cycle lengths as compared to the original attractor. This is reflected by the correlation integrals shown in Figure 7a, where the scaling region is of minor quality. Figure 7b displays the corresponding slope values. They saturate only at high values of the embedding dimension, and the saturation value of 2.027 ± 0.002 differs from the original time series.

It may be argued that those values of the burst phase where the oscillations and the discontinuity are observed are rather unphysiological: In the intact cardiovascular system, the contraction of the heart produces a pressure wave that stimulates the aortic baroreceptors. The afferent nerve stimulation is transduced in the medulla oblongata into efferent parasympathetic nerve activity, which eventually results in acetylcholine release at the cardiac vagal nerve endings. The burst phase is thus determined by the latency times of the described system and does not achieve values that provoke cycle length oscillations. We therefore ran a simulation where these values of the burst phase were forbidden. The resulting cycle lengths then exhibited undistorted scaling behavior, and the correlation dimension assumed a value of $D_2 = 1.954 \pm 0.001$, which is nearly identical to the value of $D_2 = 1.942 \pm 0.002$ achieved for the original attractor.

Conclusions

We have investigated the transfer of information from parasympathetic activity to the cycle lengths of a single sinus node cell in a numerical model. Our model is a simplification of the physiologic situation with respect to three points: First, effects resulting from the mutual entrainment of the numerous cells in a complete sinus node are neglected in using the single-cell approach. Second, we have compensated for the discrete nature of vagal burst stimulation in a rather crude way by reducing the amount of acetylcholine per stimulus in the respective simulations. Third, since no data is available on the interplay of the burst phase, stimulus delay, and number of stimuli, we had to artificially separate these parameters. Taking these limitations into account, we are still able to draw some general conclusions from our results. In general, the dynamic constants of the cardiovascular autonomic control are not conserved by the sinus node cell. Hence, it is generally not possible to reconstruct the phase space of the autonomic control from the cardiac cycle lengths. However, we have found areas in parameter space where the information on the dynamics of the cardiovascular control is mapped one-to-one onto the cycle lengths. The information encoded in the delay between subsequent stimuli within one burst, the information encoded in the burst phase, and the information encoded in the number of stimuli at constant delay is essentially conserved by the sinus node cell. On the other hand, we have shown that the attractor is significantly distorted when the number of pulses is modulated during constant total duration of the burst. This means that the sinus node is a non-trivial part of the cardiovascular autonomic control. All measurements of heart rate variability thus reflect the dynamics of not only the autonomic control, but also the sinus node.

References

[1] Heart rate variability. Standards of measurement, physiological interpretation, and clinical use. Task Force of the European Society of Cardiology and the North American Society of Pacing and Electrophysiology. Eur Heart J. 1996; 17: 354-381.

[2] Malliani A, Pagani M, Lombardi F. Methods for assessment of sympatho-vagal balance. In: Levy MN, Schwartz, PJ (editors). Vagal Control of the Heart: Experimental Basis and Clinical Implications. Armonk, NY: Futura. 1994: 433-454.

[3] Malik M, Camm AJ. Heart rate variability: From facts to fancies. JACC. 1993; 22: 566-568.

[4] Cerati D, Schwartz PJ. Single cardiac vagal fiber activity, acute myocardial ischemia, and risk for sudden death. Circ Res. 1991; 69: 1389-1401.

[5] Dokos S, Celler B, Lovell N. Ion currents underlying sinoatrial node pacemaker activity: A new single cell mathematical model. J Theor Biol. 1996; 18: 245-272.

[6] Dokos S, Celler BG, Lovell NH. Vagal control of sinoatrial rhythm: A mathematical model. J Theor Biol. 1996; 182: 21-44.

[7] Mackey MC, Glass L. Oscillation and chaos in physiological control systems. Science. 1977; 197: 287-289.

[8] Hodgkin AL, Huxley AF. A quantitative description of membrane current and its application to conduction and excitation in nerve. J Physiol. 1952; 117: 500-544.

[9] Press WH, et al. Numerical recipes in C: The Art of Scientific Computing. Cambridge: Cambridge University Press. 1992.

[10] Grassberger P, Procaccia I. Characterization of strange attractors. Phys Rev Lett. 1983; 50: 346-349.

[11] Takens F. Detecting strange attractors and turbulence. In: Rand DA, Young LS (editors). Dynamical Systems and Turbulence. Berlin: Springer-Verlag. 1981: 366-381.

Contact
Dr. Tobias Bieberle
Zentralinstitut für Biomedizinische Technik
Friedrich-Alexander Universität Erlangen-Nürnberg
Turnstrasse 5
D-91054 Erlangen
Germany
Telephone: +49 9131 8924 302
Fax: +49 9131 8924 599
E-mail: tbieberle@biomed.uni-erlangen.de